

# Progress of the X-Com project and PhD research - Report 4



Produced by:

John Atkinson, PhD Researcher, [atkinsonj@bournemouth.ac.uk](mailto:atkinsonj@bournemouth.ac.uk)

Dr Luciana S. Esteves, Associate Professor, [lesteves@bournemouth.ac.uk](mailto:lesteves@bournemouth.ac.uk)



[Faculty of Science and Technology](#)

Bournemouth University

Talbot Campus, Poole, Dorset, BH12 5BB, UK

Phone: +44 (0) 1202 9 62446

**28<sup>th</sup> November 2017**

## CONTENTS

---

Abbreviations .....	2
Acknowledgement of Funding Sources .....	2
1 Introduction .....	3
2 Methods.....	3
2.1 Changes in nearshore bathymetry.....	3
2.2 Validation of depth derived from the radar data .....	4
3 Results.....	8
3.1 Changes in Nearshore Bathymetry .....	8
3.2 Validation of Depths Derived from Radar Data .....	11
3.2.1 Validation using 40-m grid cell size.....	13
3.2.2 Comparing the depth values along selected transects.....	15
4 Summary .....	17
5 Further Work.....	18
6 References .....	18
Appendix 1 – Multibeam Survey Coverage.....	19
Appendix 2 – Effects of Wave Direction on Data Quality .....	20
Appendix 3 –Considering The North and South Sectors Independently .....	22

## ABBREVIATIONS

---

<b>BODC</b>	British Oceanographic Data Centre
<b>DGPS</b>	Differential Global Positioning System
<b>DirP</b>	Peak period direction (degrees)
<b>EA</b>	Environment Agency
<b>Hs</b>	Significant wave height (metres)
<b>LSR/L</b>	Least Square Regression /Line
<b>MCA</b>	Maritime and Coastguard Agency
<b>Metocean</b>	Meteorological and oceanographical
<b>MWL</b>	Mean Water Level (metres)
<b>NOC</b>	National Oceanography Centre
<b>ODN</b>	Ordnance Datum Newlyn (metres)
<b>SCDC</b>	Suffolk Coastal District Council
<b>X-Com</b>	X-band radar and evidence-based Coastal Management decisions

## ACKNOWLEDGEMENT OF FUNDING SOURCES

---

X-band radar and evidence-based coastal management decisions (X-Com) was a project funded by the Natural Environment Research Council (reference NE/M021564/1). X-Com partners and collaborators include: Bournemouth University (BU), National Oceanography Centre (NOC), Suffolk Coastal District Council (SCDC), Mott MacDonald, Cefas and residents of Thorpeness. The radar data analysed in the progress reports were collected during the X-Com project, while fieldwork surveys are part of a PhD studentship co-funded by Bournemouth University, Suffolk Coastal District Council and Mott MacDonald.

## 1 INTRODUCTION

---

This document is the fourth report summarising the data collection and preliminary results of the PhD research undertaken in association with the X-Com project. The first report (31<sup>st</sup> January 2017) presented an overview of data types and methods of data collection and analysis. The second report (31<sup>st</sup> May 2017) presented preliminary results of changes in nearshore bathymetry (radar data), beach topography (DGPS surveys) and cliff retreat (laser scans) south of the Ness. The third report (10<sup>th</sup> August 2017) described changes in beach topography (DGPS surveys and data provided by the Environment Agency, EA profiles) and bathymetry around the Ness (derived from X-band radar data, processing version 26<sup>th</sup> June 2017). All elevations and water depths are reported relative to Ordnance Datum Newlyn (ODN).

Using data from two multibeam surveys provided by the EA and the Maritime and Coastguard Agency, this report investigates changes in nearshore bathymetry between the summer 2014 and the winter 2017. The report also presents the validation of the radar derived bathymetry using data collected concomitantly with the bathymetric survey obtained in the winter 2017. Data validation is required to determine the accuracy of the bathymetry extracted from radar data under different wave conditions. The analysis of bathymetric changes between the two multibeam surveys provides an indication of the magnitudes of change that can be expected in the study area and the associated spatial variability. It is anticipated that this information will help identify areas where sediment may be more mobile (identified by larger changes in water depth) and areas of bed stability (identified by little or no changes in water depth).

## 2 METHODS

---

### 2.1 CHANGES IN NEARSHORE BATHYMETRY

Changes in nearshore bathymetry were quantified comparing two multibeam surveys obtained in the summer 2014 and the winter 2017 (Figure 1) by the EA and the Maritime and Coastguard Agency (MCA), respectively. The surveys' coverage extends further east in the central sector in 2014 and further north in 2017. Changes in bathymetry were calculated only for the areas covered by both surveys.

To enable comparison, data were referenced to OSGB36 coordinate system, using Ordnance Survey software GridInquest version 7.0, and ODN datum using the correction (Chart Datum -1.5 m) for Lowestoft (BODC, 2017). Using linear interpolation, data from the multibeam surveys were represented in a 0.5-resolution grid. In cases where grid cells contained more than one data point, the arithmetic mean depth value was calculated. At any given cell negative values from this analysis reflect an increase in depth between 2014 and 2017 and positive changes reflect a reduction in depth.

To extend the temporal coverage of the analysis and to obtain a better understanding of the magnitudes of change, variations in nearshore bathymetry were examined along three EA long-term shore-normal monitoring profiles (SO36, SO37 and SO38, Figure 1). Additionally, bathymetric data was extracted from the two multibeam surveys along a fourth transect (SO37.5, Figure 1) to demonstrate the variations in areas where changes were more prominent. The profile locations, data sources and dates are presented in Table 1.

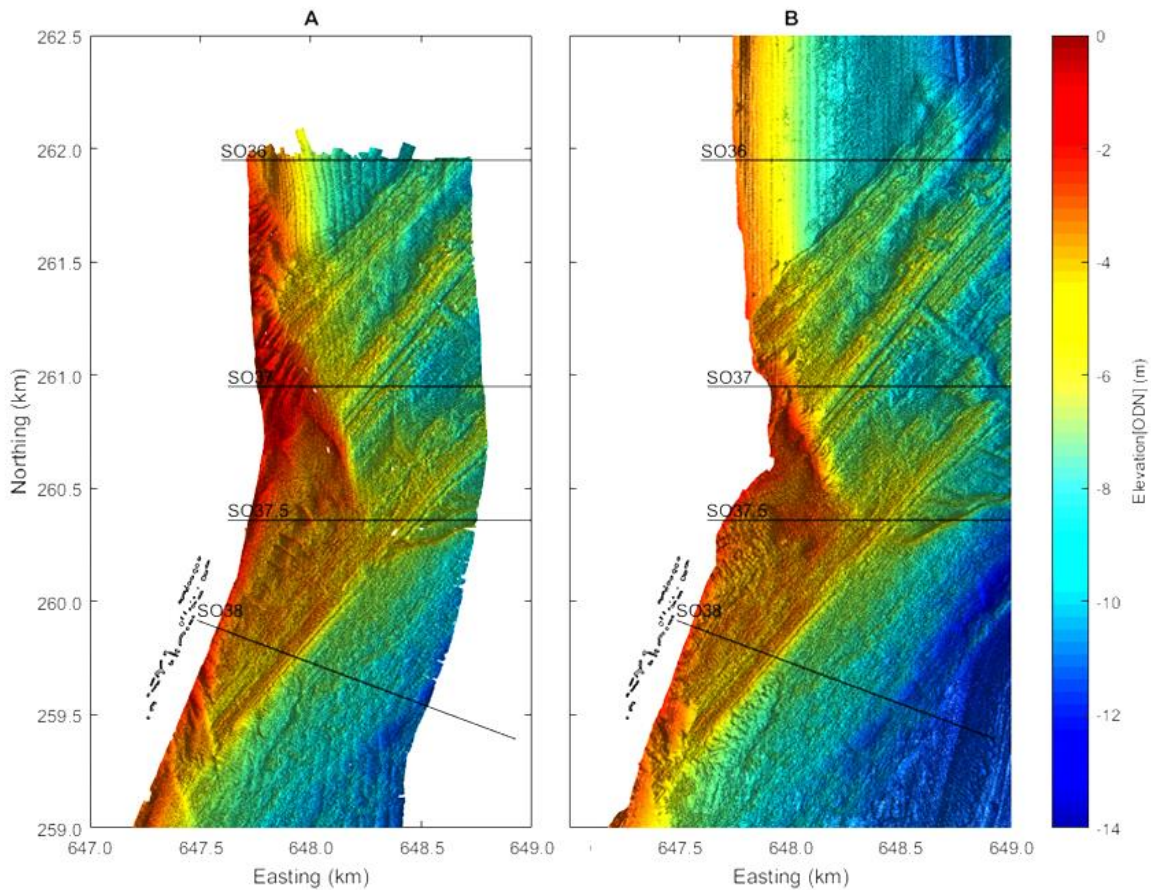


Figure 1. Bathymetry data from two multibeam surveys covering the study area: (A) obtained by the EA in July 2014 and (B) obtained by the MCA in January 2017. Both images show the position of Thorpeness buildings and the transects along which changes in bathymetry were analysed.

Table 1. Profiles coordinates (OSGB36), azimuth and data sources and dates used in the analysis of bathymetric changes.

Profile	Starting Northing	Starting Easting	Azimuth	Survey Dates	Data source
SO36	261948.10	647592.71	90°N	Aug 1992, 1997, 2007	EA profiles
SO37	260948.91	647634.85	90°N	Jul 2014	EA multibeam survey
SO38	259917.18	647484.50	110°N	Jan 2017	MCA multibeam survey
SO37.5	260358.91	647634.85	90°N	Jul 2014 Jan 2017	EA multibeam survey MCA multibeam survey

## 2.2 VALIDATION OF DEPTH DERIVED FROM THE RADAR DATA

Validation of depths derived from radar data requires actual measurements of depth in areas within the radar field of view, preferably concomitantly with radar data recording. Bathymetric (multibeam) surveys commissioned by the MCA were undertaken in the periods 30<sup>th</sup> January to 24<sup>th</sup> February 2017 in the north sector of the radar view and 7<sup>th</sup> January to 15<sup>th</sup> February 2017 in the south sector (see Appendix 1). These data became available in September 2017 and were used to validate the depths derived from radar data acquired during the same period.

Validation was undertaken using the radar data recorded concomitantly with the multibeam survey period and when wave conditions provided the best possible conditions for the estimation of depth using the radar data analysis algorithms described in Bell (1999; 2009a; 2009b). Two criteria were used to ensure the

best possible data were used in the analysis: (a) the variability of the actual bathymetry within each radar grid cell required quantification with respect to the mean, maximum or minimum depth values before undertaking a correlation analysis to identify which of these three values should be used in the validation process; and (b) identification of the wave conditions most suitable to derive the most accurate radar estimates of depth during the survey period.

Multibeam surveys measure bathymetry at a higher spatial resolution (0.5 to 1.0m) than the cell size (60 x 60m) used to extract depth from radar data. Therefore, it is necessary to analyse the data from the multibeam surveys using a grid with the same domain and resolution as the radar data (Figure 2). For each radar grid cell, the minimum, maximum, mean, standard deviation and range of depth values were calculated (Figure 3). These values were then compared with the depth derived from the radar data (through linear regression) to determine the best value to use in the validation process. Both the 'depth memory' method to estimate depth from radar records, and the cell size resolution used here were established by the NOC during the X-Com project.

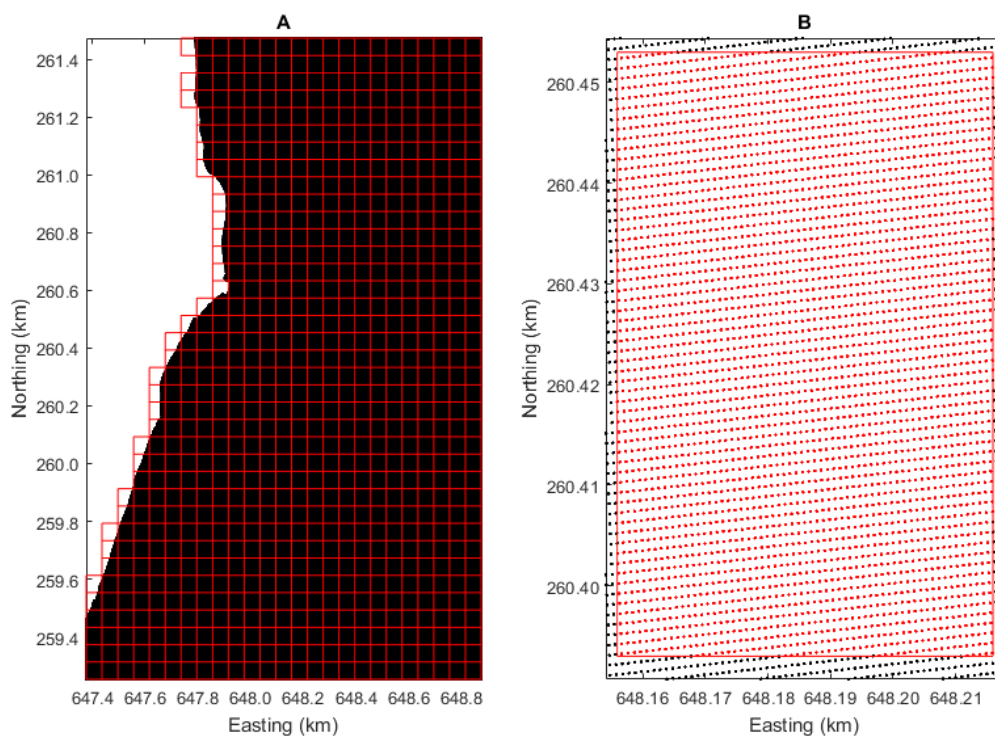


Figure 2. (A) Data points of the multibeam survey are shown in black and the radar grid is shown in red. (B) The multibeam data points confined within a grid cell boundary (identified in red) are used to calculate the values that will represent that cell in the validation process.

High standard deviation values (Figure 3D) define the cells with the largest bathymetric variation (up to 4m). Visual inspection of the multibeam data showed that high standard deviation values usually reflected steeper slopes and/or the edge of features, such as the Coralline Crag ridges or large bedforms (sand waves). The accuracy of the bathymetry derived from radar data can be affected in areas of complex bathymetry, particularly where depth increases or decreases sharply within a grid cell. Assuming uniform wave behaviour across the area, depth values are estimated as a function of the changes in wave period and wavelength as waves interact with the seabed. Non-uniform changes in depth cause non-linear effects on the wave field. These interactions are not captured by the radar or in the formulations used in the data processing and thus contribute to errors in radar-derived bathymetry.

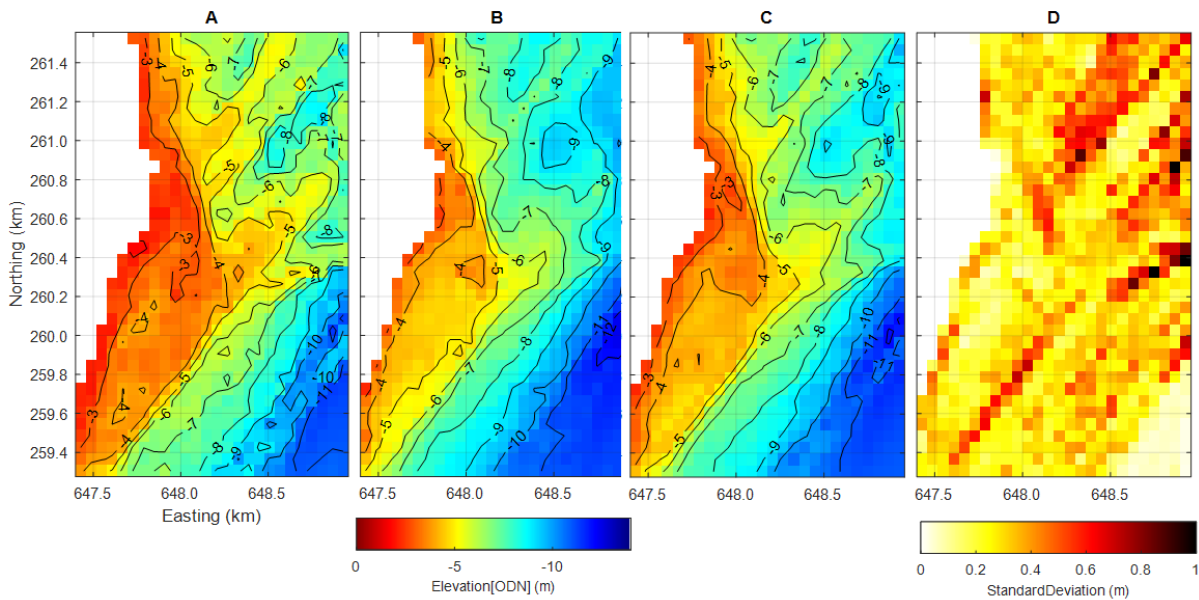


Figure 3. Maps produced using the (A) minimum, (B) maximum, (C) mean depth values and (D) standard deviation of multibeam data points for each cell in the radar grid.

The depth values estimated from each radar record in the period from 1200 7<sup>th</sup> January to 1200 24<sup>th</sup> February 2017 were compared with the minimum, maximum and mean depth values of the multibeam survey data for the respective grid cells. Positive, reasonably strong correlation ( $R^2 > 0.64$  for all values) and statistically significant ( $p < 0.05$ ) linear relationships exist between the radar-derived depths and the minimum, maximum and mean values of the depth measurements. Throughout the period of analysis the maximum depth values show the strongest correlation with the radar-derived depths as demonstrated by the highest correlation coefficients (Table 2 and Figure 4). Therefore, in the following sections, the maximum depth values are used in the validation process.

The sharp decrease in  $R^2$  values observed between the 25<sup>th</sup> January and 9<sup>th</sup> February (Figure 4) indicates poorer agreement between radar-derived depth and survey measurements. The accuracy of the ‘depth memory’ method used to derive bathymetry is observed to slowly degrade during periods in which wave heights are lower than 1.0 to 1.5m, and wave direction tends to be southerly or variable. On the other hand, accuracy improves when waves approach from the northeast with heights greater than 1m. The duration in which wave conditions persist also influence the accuracy of the estimated depth as the ‘depth memory’ method uses data averages over a variable period of time. Appendix 2 presents further analysis related to the effect of wave direction on data quality.

Table 2. Minimum, mean and maximum correlation coefficient values ( $R^2$ ) obtained from linear regression between radar-derived depths and the mean, minimum and maximum values of the depth measurements within the corresponding radar grid cell.

	$R^2$ values		
	Minimum	Mean	Maximum
<b>Mean Depth</b>	0.68	0.86	0.95
<b>Minimum Depth</b>	0.64	0.84	0.92
<b>Maximum Depth</b>	0.73	0.87	0.95

Figure 5 shows the radar derived wave conditions during the multibeam surveys. Between 23<sup>rd</sup> January and 7<sup>th</sup> February the radar data show rapid changes in the direction and period in consecutive records, which contributes to ‘noise’ in the data. Data ‘noise’ often results from the inability of the radar to accurately register waves smaller than 1m, and is reflected in the reduction of  $R^2$  values (Figure 4). Conversely, between 7<sup>th</sup> and 23<sup>rd</sup> January 2017 there is much less ‘noise’ in the data, indicating optimum wave conditions for obtaining radar-derived depth. This is confirmed by  $R^2$  values close to, or above, 0.9 (Figure 4).

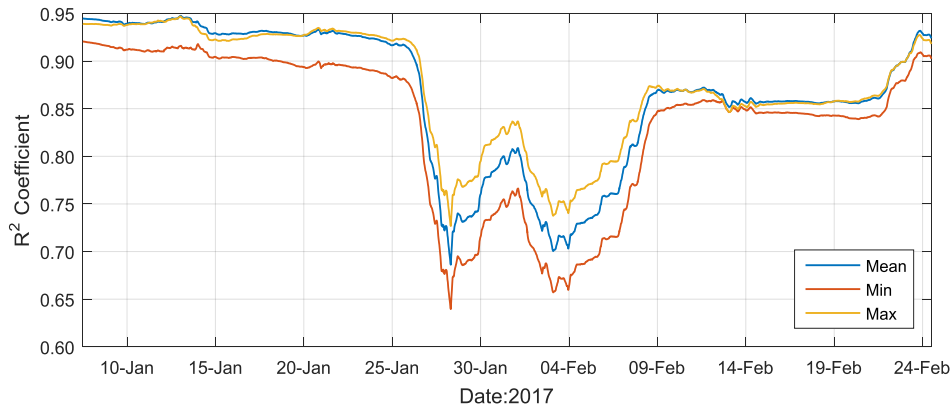


Figure 4. Correlation coefficient ( $R^2$ ) values obtained from linear regression between the depth estimated from each radar record in the survey period and the mean, minimum and maximum measured depths for the equivalent grid cell.

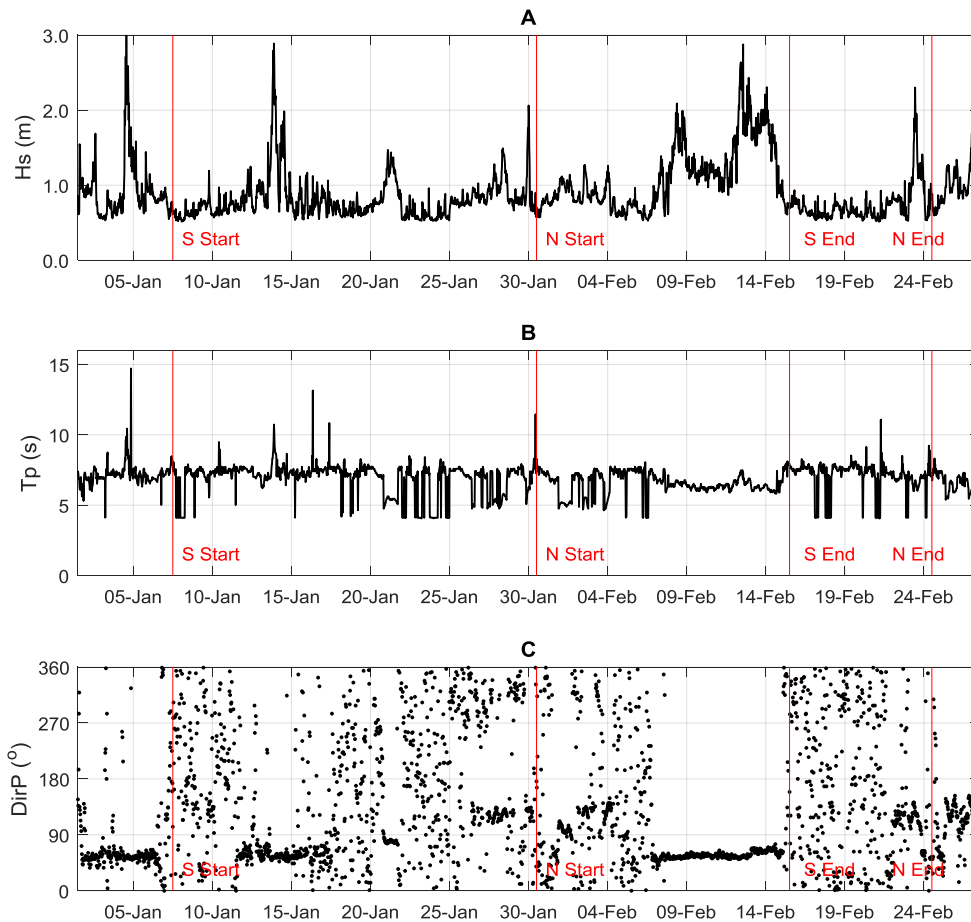


Figure 5. Radar derived significant wave height (A), peak period (B) and peak direction (C) during the period of the multibeam surveys. Red lines indicate the start and end of surveys covering the north and south of the radar view.

The highest  $R^2$  value was found for the correlation between the maximum measured depth and the estimated depth extracted from the radar data recorded on 0230 13<sup>th</sup> January 2017 (the radar derived bathymetric map is shown in Figure 6a). The least-squares regression line (LSRL) equation for this period was calculated and rearranged to 'calibrate' the radar-derived depths (equation 1).

$$x = (y - c)/m \quad (1)$$

Where  $c$  is the value of the LSRL intercept at the vertical axis,  $m$  is the slope of the LSRL,  $y$  is the uncalibrated radar-derived depth and  $x$  is the calibrated radar-derived depth.

To assess how the spatial resolution (the size of the grid cell) impacted on the accuracy of the radar-derived depth values during the optimum wave conditions, the validation procedure described above was repeated using a 40m grid cell size. Following 13-days of depth memory processing to ensure the data signal was stable, depths were extracted from the radar data recorded at 0230 13<sup>th</sup> January 2017 and were compared with data obtained previously at a lower spatial resolution (60m cell size). The radar-derived bathymetric map for the 40m grid resolution is shown in Figure 6b. Differences of 2m and 1m are observed in the nearshore and offshore areas, respectively, with the higher resolution 40m data generally indicating shallower depths than the 60m data (Figure 6).

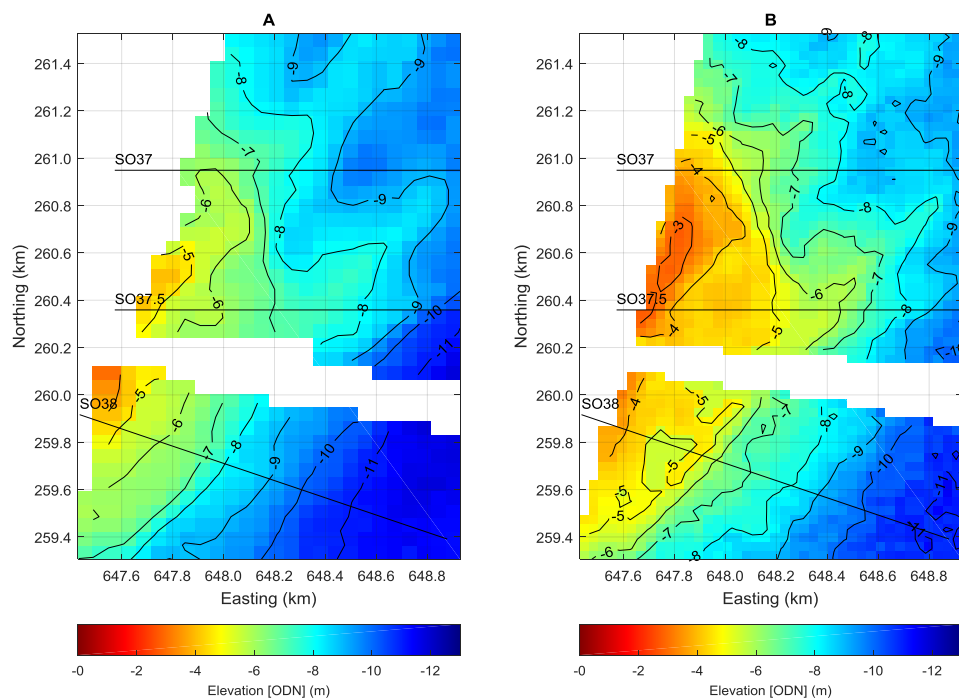


Figure 6. Bathymetric maps produced from radar data recorded on 0230 13<sup>th</sup> January 2017 with depths extracted with (A) lower spatial resolution (60m grid cell) and (B) higher spatial resolution (40m grid cell).

## 3 RESULTS

### 3.1 CHANGES IN NEARSHORE BATHYMETRY

Coralline Crag ridges aligned SW/NE are evident in both multibeam surveys (Figure 1) and exhibit little or change in bathymetry between the two surveys. In fact, areas showing no or little change in bathymetry dominate across the entire study area, except in areas closest to the shore and in the central sector (Figure 7). The largest changes reflecting erosion of around 3m are observed closer to the shore north and south of the Ness, including the frontage along Thorpeness. The data show a dominance of accretion around the Ness and at the centre of the study area.

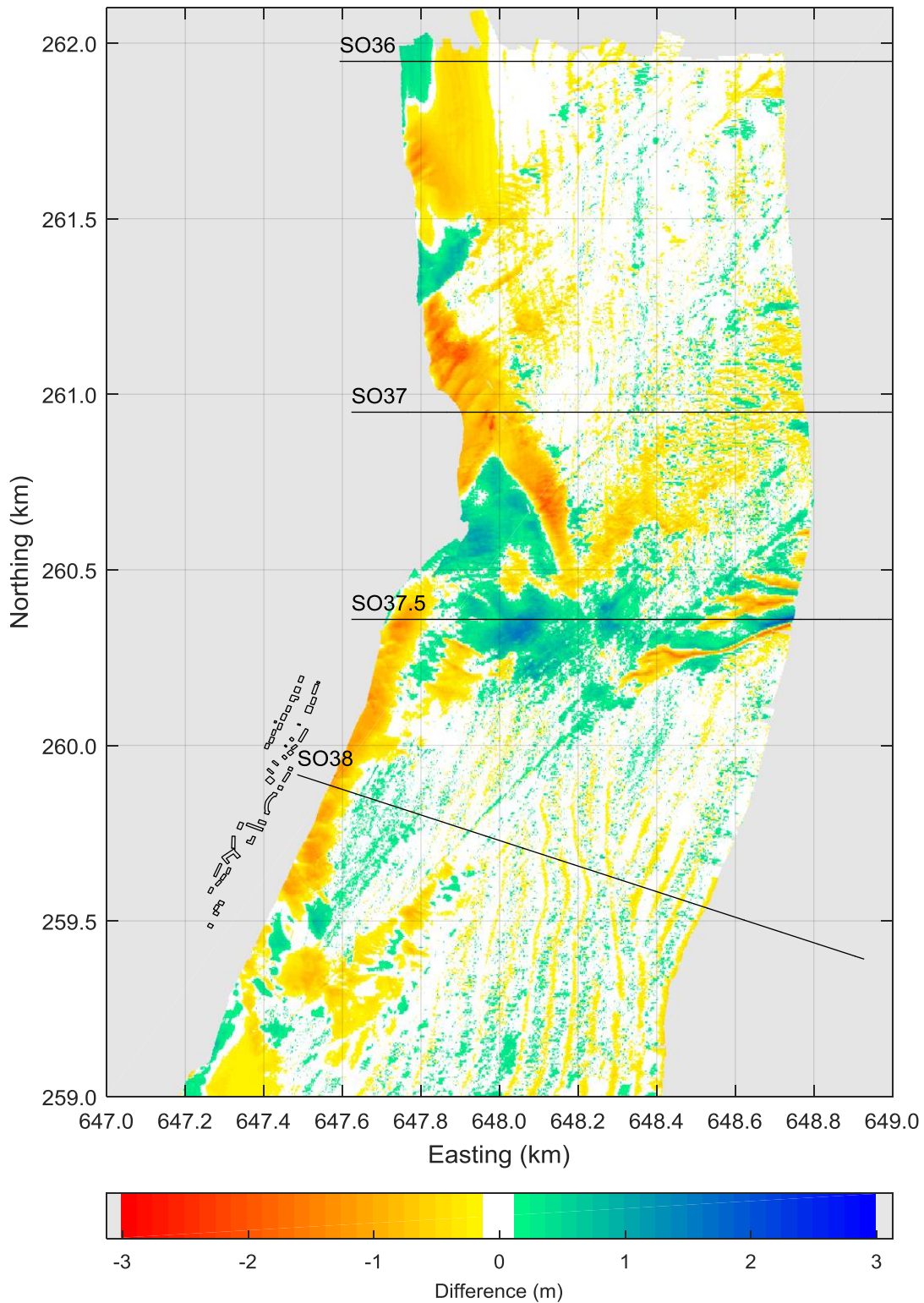


Figure 7. Difference in the depths recorded between the 2014 and 2017 surveys. Negative values indicate an increase in depth (usually due to sediment loss) and positive values indicate a reduction in depth (usually due to sediment gain). Areas in white represent changes within  $\pm 0.125\text{m}$ . Transects analysed in this report are indicated as black lines.

Alternating bands of deposition and erosion are visible offshore of the central sector (more prominently along SO37.5 and less so along SO37). These features are interpreted as large bedforms, probably sand waves. The northern position of these large bedforms appears to be controlled by the underlying geology, as evidenced by a band of accretion  $< 1\text{m}$  aligned with the Coralline Crag ridges. This pattern of alternating erosion and accretion bands suggests a north-westerly migration of large (2m high) bedforms, such as sand

waves, although confirmation requires further investigation. The migration of these bedforms reflects the largest changes observed in offshore areas, evident in transect SO37.5 (Figures 8C), which may be driven by the dominant southerly high wave energy ( $H_s > 2.5\text{m}$ ) observed between 2014 and 2016 (see Progress Report 2).

Unlike the features described above, which seem to reflect actual dynamic bedforms, bands of erosion ( $< 0.5\text{m}$ ) aligned approximately north-south in the southwest and less pronounced in the north of the survey area (Figure 7) are believed to be artefacts of the surveying method. They seem to align with the survey lines (or the trajectory of the vessel) in 2014 (Figure 1A), and result in a band of erosion that perfectly follows the south-eastern edge of the survey coverage (Figure 7).

To better understand the magnitudes of changes that can be expected in the study area, the bathymetry measured between 1992 and 2007 along the EA long-term monitoring profiles were compared with the data obtained from the two multibeam surveys (Figure 8). Except for the 2017 survey (which was collected in January), all the profile data were collected in the summer. Here the comparison is particularly useful to assess whether depths in 2017 reflect a seasonal signal or fall within the range of the depths measured in previous years. Visual analysis of the data shown in Figure 8 indicates the latter, except in the nearshore region of profile SO38 (Figure 8D), where increased depths were measured in January 2017. This evidence indicates enhanced erosional condition not registered in previous surveys. At this location, data suggest a trend of erosion, as depths in the nearshore seem to increase from the 1990s data to 2014 and 2017. It is noted that, between 2014 and 2017, depths increased in the nearshore and decreased further offshore in the central sector (Figure 8C). Such changes reflect seasonal summer-winter changes that are common in many coasts. However, in the study area, these seasonal changes were observed only along transect SO37.5.

The largest bathymetric changes between 1992 and 2017 were observed in the nearshore region and were observed to vary by 2 to 3m at depths shallower than 6m in the north sector (Figure 8A and 8B) and up to 2m at depths shallower than 4m in the south sector (Figure 8D). The spatial distribution and magnitudes of change are similar to the values shown in Figure 7, suggesting that this is the pattern expected at seasonal or inter-annual scales. This further indicates that any major differences (such as estimates derived from radar data) should be considered with caution. Further offshore, the largest bathymetric changes reach 2m (Figure 8C) and seem to relate to the migration of large bedforms. Modelling simulations may help elucidate whether these features are indeed mobile sand waves responding to local hydrodynamic conditions.

Potential differences in the survey methods, and unknown uncertainties related to the EA data, prevent a detailed quantitative comparative analysis of radar and multibeam data. Results described here focus on general differences and patterns that can be identified with confidence after cautious considerations of the data shown in Figure 8. Issues identified with the EA data include: (a) the 1997 survey seems to have lower resolution as it lacks some of the bathymetric features (likely the Coralline Crag) consistently present in other surveys; and (b) the 2007 survey seems to show an eastward displacement of features when compared with the other surveys, which may suggest an issue with the coordinate system or the geoid projection. Nevertheless, the presence of stable features defined by the underlying geology gives confidence in the general interpretations presented in this section.

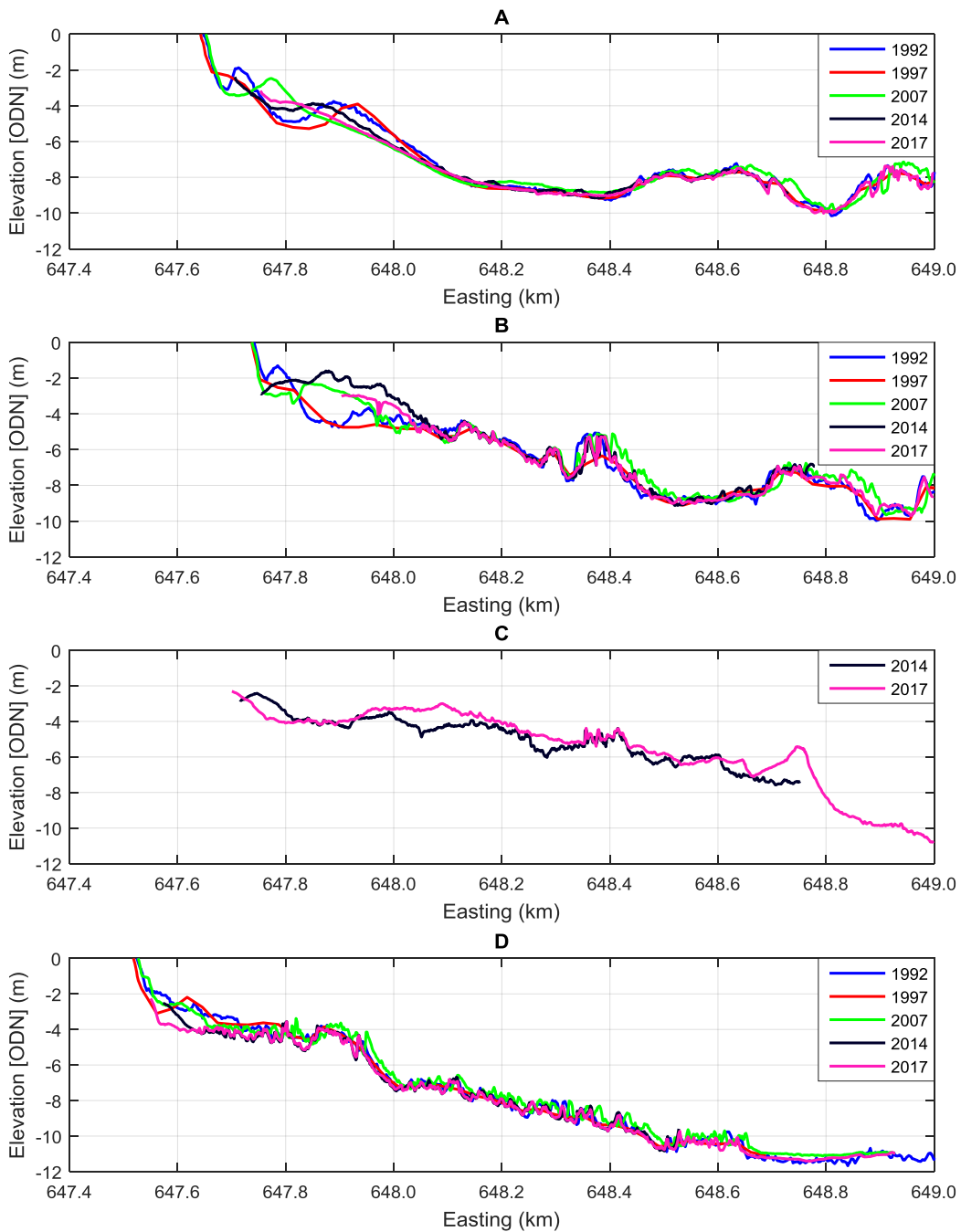


Figure 8. Bathymetry measured in the summer of 1992, 1997 and 2007 (EA long-term monitoring) and the summer of 2014 and winter of 2017 (multibeam surveys commissions by the MCA) along the four selected transects (A) SO36, (B) SO37, (C) SO37.5, (D) SO38. Mean sea level at Thorpeness is estimated to be -0.16m ODN. Note that the azimuth of profile SO38 is 110°N, while all others have azimuth of 90°N.

### 3.2 VALIDATION OF DEPTHS DERIVED FROM RADAR DATA

The linear regression results for the maximum measured depth at each 60m radar grid cell, and the respective uncalibrated and calibrated radar-derived depth (extracted from the radar record of 0230 11<sup>th</sup> January 2017) are presented in Figure 9A and 9B, respectively. The calculated residuals for both uncalibrated and calibrated values are shown in Figure 9C. Analysis of the uncalibrated data indicates that the radar data processing tends to over-estimate depths, with the accuracy of the results decreasing in shallower areas where residuals reach 3m.

In deeper waters (where water depth,  $d$ , is greater than half the wavelength,  $\lambda$ :  $d > \lambda/2$ ), linear wave theory is usually adequate to model wave propagation. However, in shallow waters ( $d < \lambda/2$ ), wave transformations are non-linear and more complex to model. If radar data processing algorithms are based on linear wave theory, some improvement in the accuracy of the radar-derived depths in shallow water may be achieved through nonlinear wave theory formulations.

Following the radar calibration process described above, the accuracy of radar-derived depths increases: (a) grid cells showing estimated depths within  $\pm 0.5\text{m}$  of the maximum measured depth increase from 48% to 77%; and (b) grid cells showing estimated depths within  $\pm 1\text{m}$  of the maximum measured depth increase from 73% to 94% (Figure 9D, E). Figure 10 shows bathymetric maps produced using the maximum depth measured within each 60- grid cell (panel A), uncalibrated radar data (panel B top) and calibrated radar data (panel B bottom) and the resulting differences between measured and estimated depths (panel C). Calibration has clearly improved the accuracy of the estimated depths across the radar view. However, the calibration is observed to increase errors in parts of the nearshore, with overestimated depth nearest the shoreline and underestimated depths further offshore.

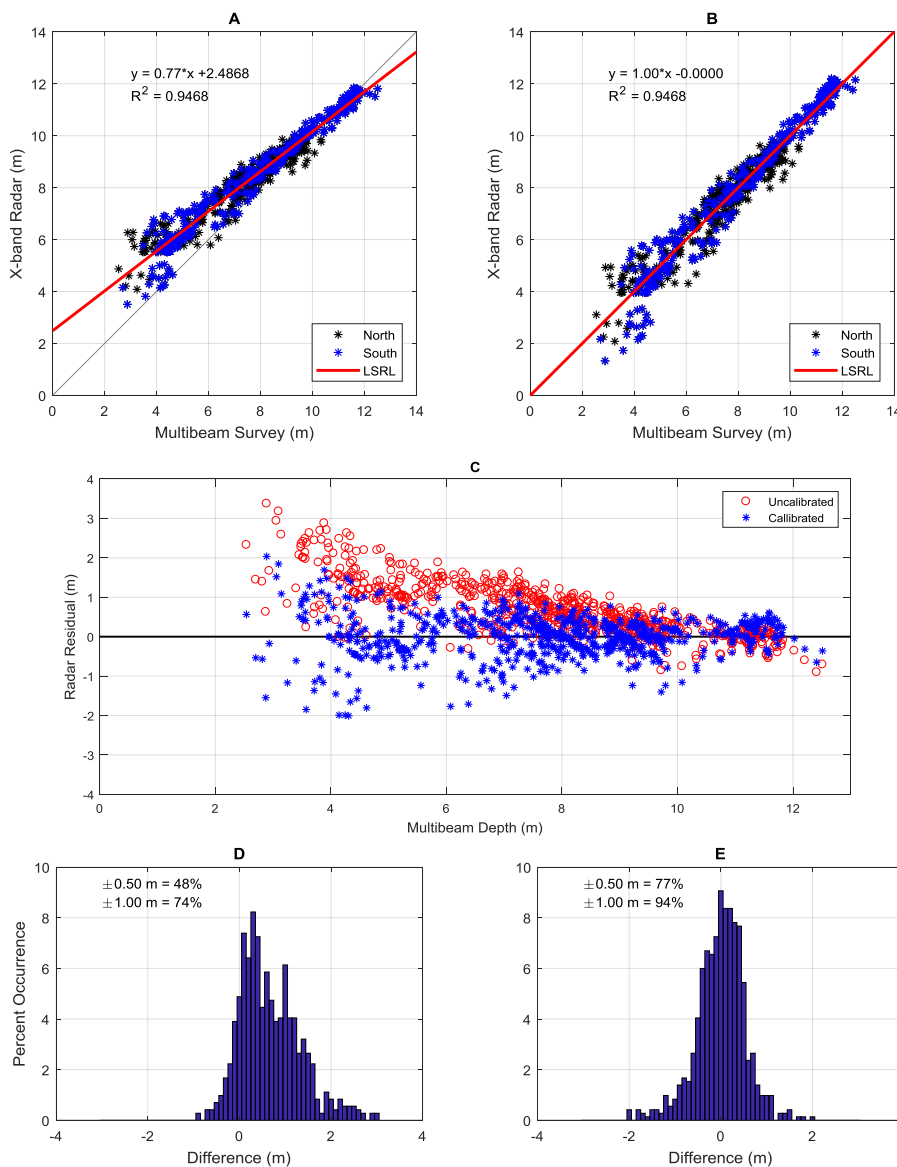


Figure 9. Linear regression correlation coefficient ( $R^2$ ) for maximum depth measurements obtained from the 2017 multibeam surveys at 60-m grid resolution compared with uncalibrated (A) and calibrated (B) radar-derived depth for data recorded on 13-Jan-2017 02:30; uncalibrated and calibrated data residuals (C) and their respective frequency distribution (D and E).

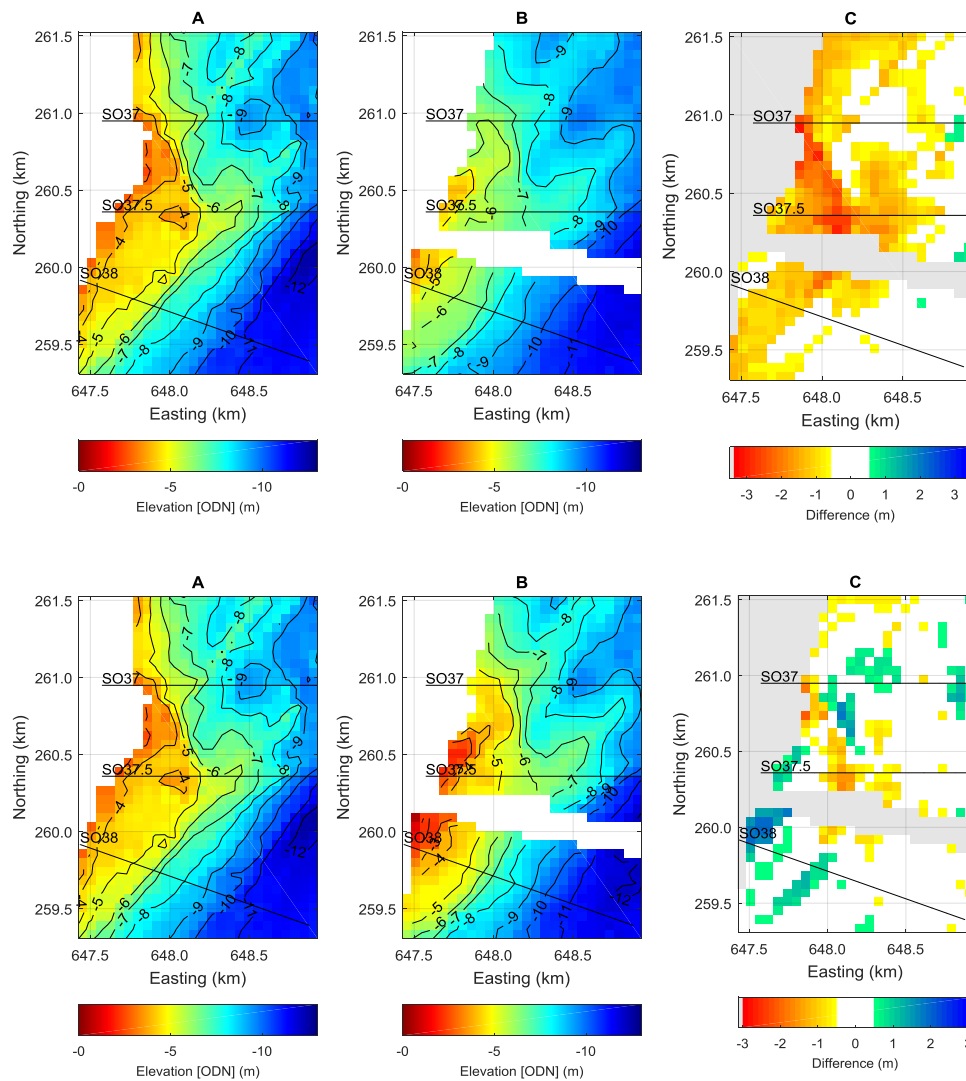


Figure 10. Bathymetric maps showing: (A) the maximum depth measured within each 60-m grid cell; (B) top) uncalibrated and (B bottom) calibrated radar-derived depth (13-Jan-2017 02:30); and (C) the resulting differences between measured and estimated depths (white areas indicate differences of  $\pm 0.5$  m).

### 3.2.1 Validation using 40-m grid cell size

The same procedure used in the validation of radar-derived depths extracted at a 60-m grid resolution was followed in the validation of data extracted at a grid cell size of 40m. Results of the linear regression indicate that calibration does not result in considerable improvement of accuracy of the radar-derived depths (Figure 11A, B). The largest variances are around  $\pm 2$ m for measured depths around 6m. At shallower depths, accuracy is improved when compared with the data extracted at 60m grid resolution (compare Figures 9C and 11C).

The frequency distribution of the residuals confirms that calibration had no significant impact on the accuracy of estimates (Figure 11D, E). The uncalibrated data at 40m resolution (Figure 11D) showed an improved accuracy when compared with the uncalibrated data at 60m resolution (Figure 10D). However, the same is not observed for the calibrated data. Results analysed to date suggest that the best validation outcome is obtained by comparing the calibrated radar-derived depths at 60m resolution with the measured maximum depth (Figure 9). Validation results obtained using the mean measured depth and radar-derived depth for both 60m and 40m grid resolution are provided in Appendix 4.

Bathymetric maps in Figure 12 show the maximum depth measured within each 40m grid cell (panel A) of uncalibrated (panel B top) and calibrated (panel B bottom) data and the resulting differences between measured and estimated depths (panel C). Uncalibrated data provide the most accurate estimates of nearshore depth, except in the northernmost sector (Figure 12C top). Both uncalibrated and calibrated data tend to overestimate depths in the northern sector and underestimate in the southern sector. When errors are consistently positive or negative biased (dominantly over-estimating or under-estimating), an offset value could be applied to adjust values and reduce errors. This is not the case here.

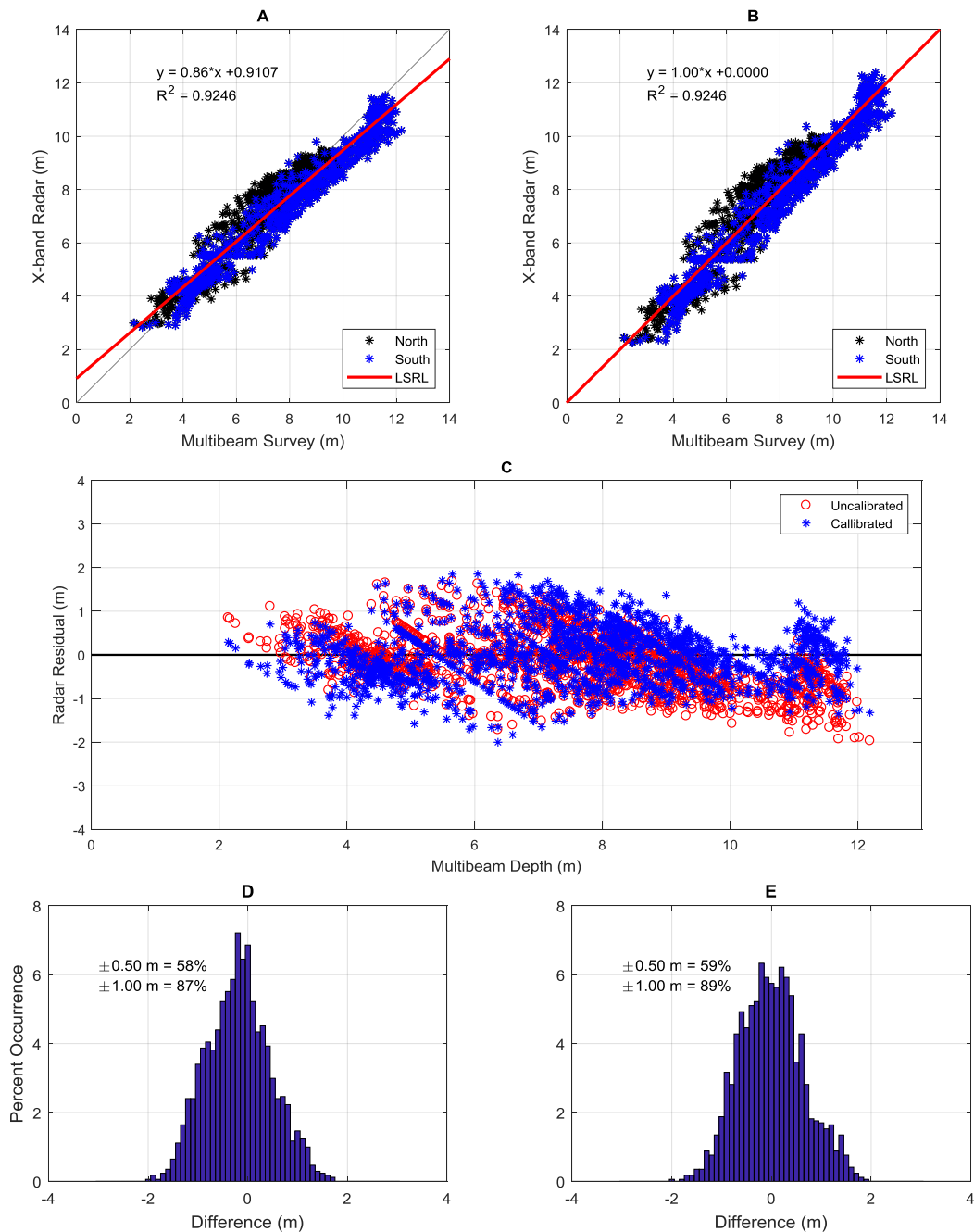


Figure 11. Linear regression correlation coefficient ( $R^2$ ) for maximum depth measurements obtained from the 2017 multibeam surveys at 40-m grid resolution compared with uncalibrated (A) and calibrated (B) radar-derived depth for data recorded on 13-Jan-2017 02:30; uncalibrated and calibrated data residuals (C) and their respective frequency distribution (D and E).

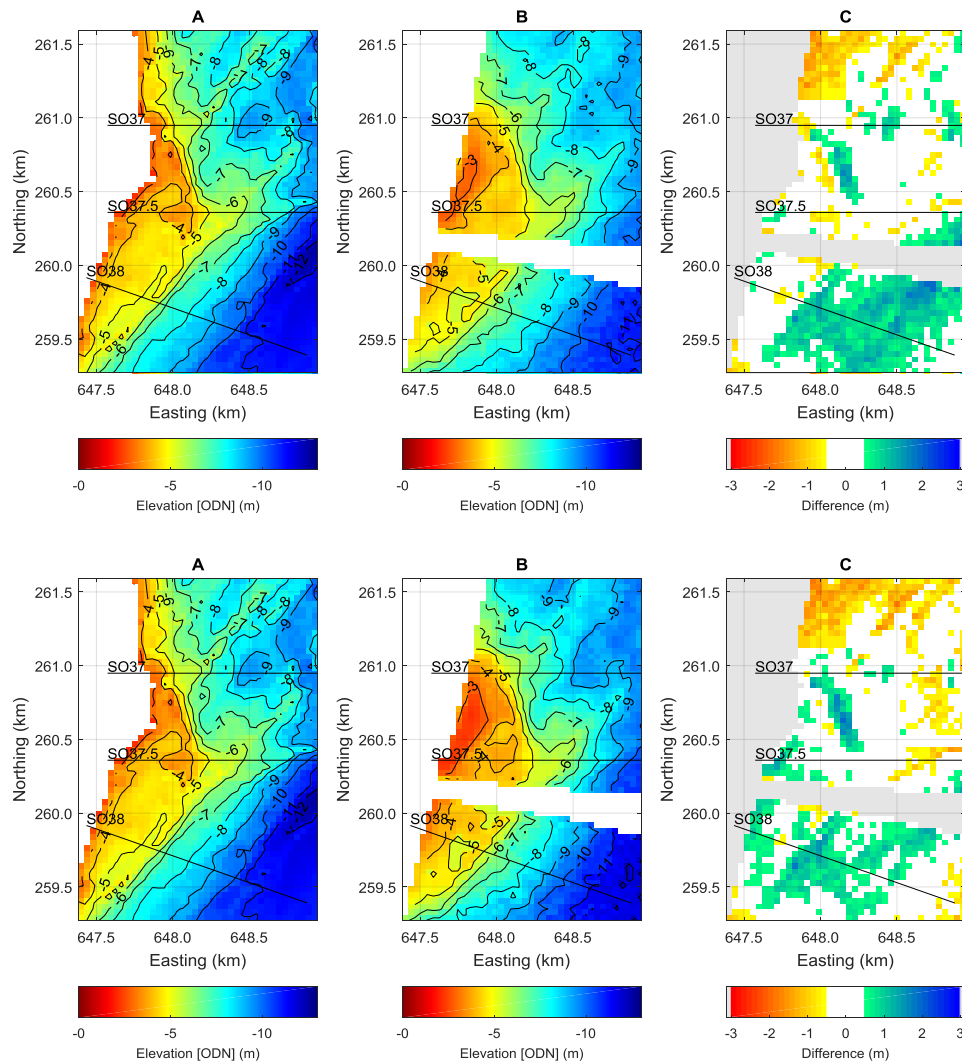


Figure 12. Bathymetric maps producing with: (A) the maximum depth measured at 40-m grid resolution; (B top) uncalibrated and (B bottom) calibrated radar-derived depth (13-Jan-2017 02:30); and (C) the resulting differences between measured and estimated depths (white indicates differences <0.5 m).

### 3.2.2 Comparing the depth values along selected transects

To better understand the differences between the measured and radar-derived bathymetry, depth values along three selected profiles were compared (Figure 13). It is important to notice that there are differences between the profiles showing maximum measured depths for the low and high grid resolution. These two profiles seem to show larger differences in the north (Figure 13A) and to be in better agreement in the south (Figure 13C). As expected, the low grid resolution does not reflect the range of bathymetric changes captured by the higher grid resolution.

Due to the accuracy of the data processing methods, and the limitations described in this report, the radar-derived profiles are smoother and less able to represent bathymetric features. All data generally show the same profile shape, with the uncalibrated, low-resolution radar data showing the greatest variance (2m) reflect in over-estimation of depth values (less so in the south, Figure 13C). As the validation results suggest, the calibrated low-resolution radar data are better correlated with the measured profiles, particularly in the north (Figure 13A) where agreement is similar to the high-resolution profiles, although it fails to reproduce prominent features in the central sector (Figure 13B). In the south (Figure 13C), the high-resolution radar data underestimates depth (1 m) along most of the profile.

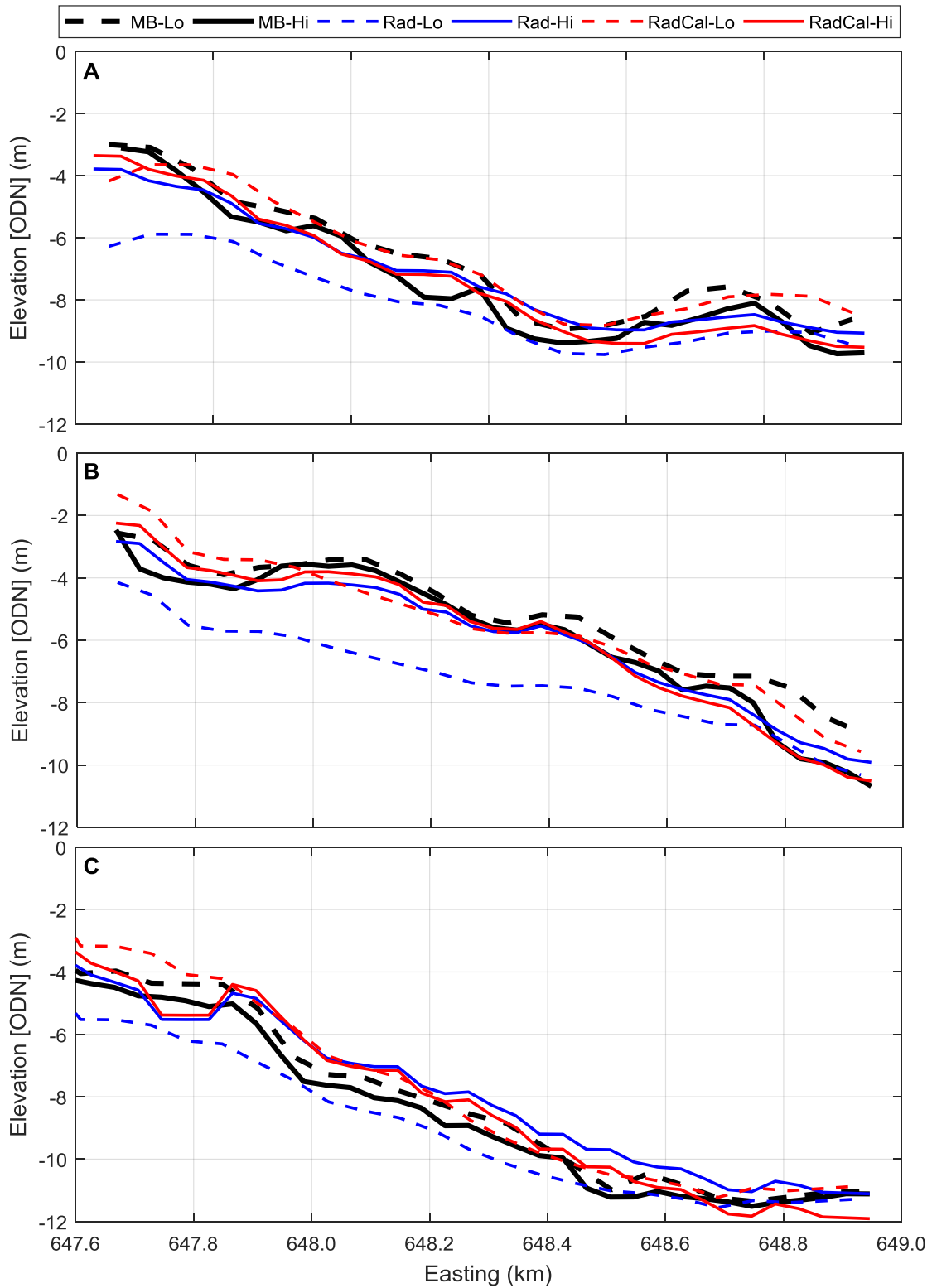


Figure 13. Maximum measured depths for grid cells of 60-m (MB-Lo) and 40-m (MB-Hi) and the equivalent calibrated (RadCal-Lo and RadCal-Hi) and uncalibrated (Rad-Lo and Rad-Hi) radar-derived depths for cells along transects (A) SO37, (B) SO37.5 and (C) SO38 of multibeam data transects (for high and low resolution) and the corresponding calibrated and raw radar derived transects.

## 4 SUMMARY

---

The analysis of bathymetric changes using survey data from the EA long-term monitoring profiles (measured in the summer of 1992, 1997 and 2007), and multibeam surveys conducted in July 2014 and in January 2017 have been used to assist understanding of the magnitudes of change and their spatial and temporal variability in the study area.

The best radar data validation outcome was obtained by comparing the calibrated depths derived from the 'best radar record' processed at 60m grid resolution with the maximum measured depth within equivalent grid cells. The accuracy of radar-derived depths obtained from this 'best validation outcome' was  $\pm 0.5\text{m}$  for 77% of the cells and  $\pm 1.0\text{m}$  for 94% of the cells (Figure 9). However, errors continue to be high ( $\pm 2\text{m}$ ) in parts of the nearshore, with overestimated depth in some cells and underestimated depths in others. Tests using an improved 40m grid resolution improved the accuracy of depth estimates in shallower water, but overall, validation results show lower accuracy than data derived using the 60m grid.

A source of uncertainty in the radar-derived depths concerns the effect of wave direction on the strength of the data signal across the radar view. Results indicate that even during best wave conditions, the strength of the signal return is variable across the radar view. Therefore, the data accuracy is spatially variable (see Appendix 2). Waves approaching from the northeast provide greater accuracy in the radar derived depths in the north sector and lower accuracy in the south which degrades with the distance from the radar. Waves approaching from the southeast will result in greater accuracy in the south and accuracy degrading in the north with increasing distance from the radar.

The key findings of data analyses presented here are:

- Most of the study area shows little or no change in bathymetry, except in the nearshore and across the central sector of the radar view (Figure 7);
- The largest changes reach magnitudes of around 3m with erosion dominating closer to the shore north and south of the Ness, including along Thorpeness, and deposition dominating around the Ness and at the centre of the study area;
- The bathymetric changes tend to be larger (up to 3m) and extend to deeper waters (to the 6m isobath) in the north sector. In the south, changes of up to 2m were observed at depths shallower than 4m.
- The nearshore region in front of Thorpeness appears to show an erosional trend with an increase in depth of almost 2m between 1992 and 2017 (Figure 8D), while little change is observed further offshore.
- In offshore areas, the most prominent changes in bathymetry reach 2m and seem to be related to the observation of large bedforms (probably sand waves) migrating northwestward in the central sector (along transect SO37.5, Figures 7 and 8C). The northern position of these bedforms seems to be controlled by the presence of the Coralline Crag ridges. The migration of these features suggest strong currents and active sediment dynamics, likely driven by the dominant southerly high wave energy ( $H_s > 2.5\text{m}$ ) observed between 2014 and 2016. These interpretations are based only on the analysis of the differences between two bathymetric surveys and need to be further investigated.
- Depths measured in the winter 2017 fall within the range of the depths measured in the summer of previous years, suggesting a weak seasonal signal. The typical summer to winter changes with depths increasing in the nearshore and decreasing further offshore was only registered in the central sector (along transect SO37.5, Figure 8C).

## 5 FURTHER WORK

---

Data validation has improved the understanding of the accuracy and limitations of the radar-derived bathymetry. This new knowledge has implications for previous interpretations of sediment dynamics and bathymetric changes presented in previous reports and a revision will be required that takes account of the new information. Specifically, it is now clear that bathymetric data with accuracy of  $\pm 1\text{m}$  can be derived from radar data obtained at specific wave conditions only. The variance in the radar-derived depths demonstrated here limits the production of bathymetric time-series and thus the types of analysis that can be undertaken based on radar data needs to be carefully considered.

Wave transformations are non-linear in shallow waters and more complex to undertake. Since present radar data processing algorithms are based on linear wave theory, some improvement in the accuracy of the radar-derived depths in shallow water may be achieved through the application of non-linear wave theory formulations. To prevent data misinterpretations due to the spatial variability in data accuracy, radar-derived bathymetry must include a clear measure of uncertainty, based on the strength of the signal or other relevant parameter. Criteria should be developed to eliminate radar-derived bathymetric data that fails to meet clearly defined data quality criteria. At present it is unclear whether improvements to the algorithms used in the 'depth memory' method can be made to effectively reduce the spatially variable in data accuracy. Alternative data processing methods may need to be explored.

## 6 REFERENCES

---

- Bell, P. S., 1999. Shallow water bathymetry derived from an analysis of X-band marine radar images of waves. *Coastal Engineering*, 37 (3–4), 513–527.
- Bell, P. (2009a) Coastal mapping around shore parallel breakwaters. *Hydro International*, 13 (1), 18- 21.
- Bell, P. (2009b) Remote bathymetry and current mapping around shore-parallel breakwaters. *In: 33rd IAHR Congress - Water Engineering for a Sustainable Environment*, Vancouver, August 9-14
- BODC (2017). *Chart datum & ordnance datum | National Tidal and Sea Level Facility*. [online]. Available at: <http://www.ntsfl.org/tides/datum> [Accessed 22 Nov. 2017].
- Gardline Geosurvey, (2017) *HI 1495 – England East Coast Survey Report*, (Internal document).

## APPENDIX 1 – MULTIBEAM SURVEY COVERAGE

The multibeam bathymetric surveys in January and February 2017 were undertaken in the areas indicated by the coloured polygons in Figure 14. The area of the radar view (identified by the red outline) was covered by two surveys. The northern sector of the radar view (the pink area) was surveyed by the vessel Titan Discovery between 30-Jan-17 and 24-Feb-17. The southern sector (the green area) was surveyed by the vessel Titan Endeavour between 07-Jan-17 and 15-Feb-17. Titan Endeavour completed surveying missing patches in the green area on 28-Feb-17, 06-Mar-17, 07-Mar-17 and 14-Mar-17.

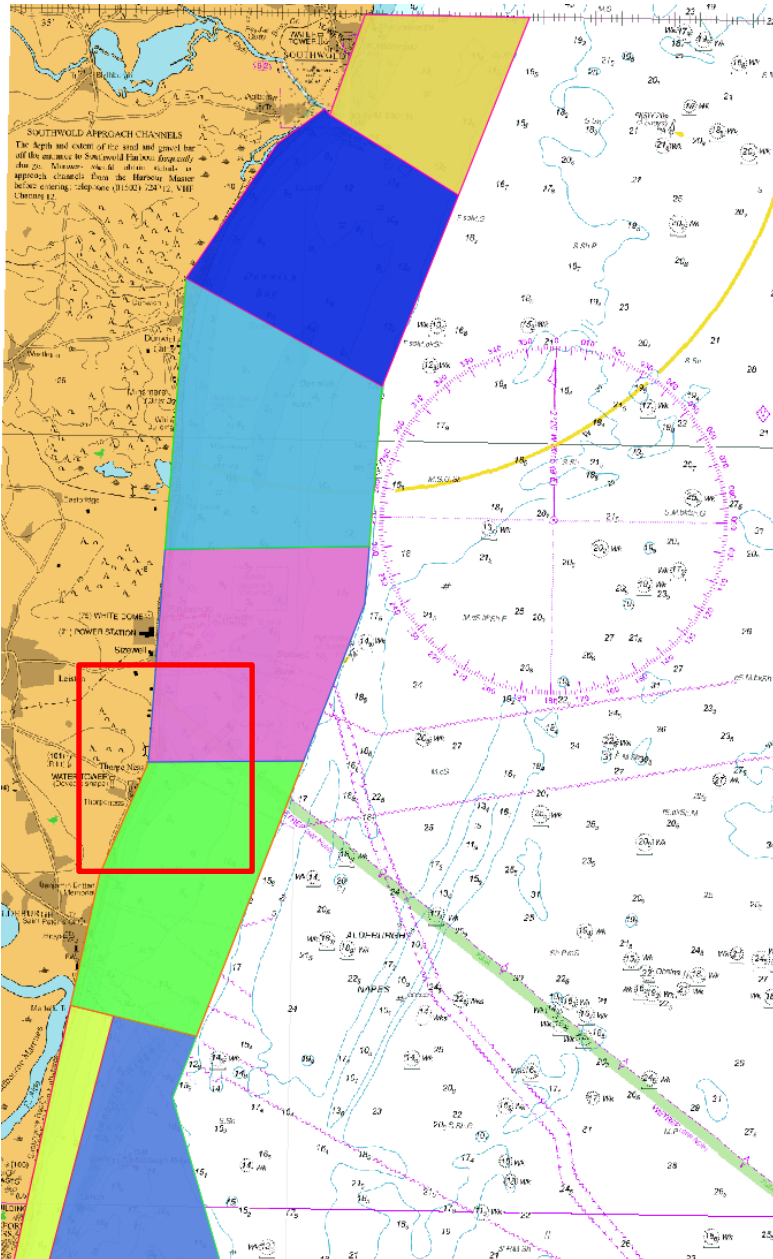


Figure 14. Areas covered by the multibeam surveys in the winter 2017 (Source: Gardline). The approximate radar view area is indicated by the red box.

## APPENDIX 2 – EFFECTS OF WAVE DIRECTION ON DATA QUALITY

The radar-derived depths estimated for each cell in the north and south sections over the respective survey periods ranged up to 4m (Figure 15). The largest variations were observed in the SE section, an area where existing data suggest relative stability. It is considered that the variance probably reflects poor data quality due to a combination of low wave conditions and the relative greater distance from the radar. Radar-derived depth changes exceeding 2.5m are observed in the NE section of the radar view. These data are likely to be influenced by the distance from the radar and a complex but stable bathymetry within the radar cells (sharp changes in depth due to the presence of Coralline Crag ridges). In both areas, it is highly unlikely that this variance in depth reflects actual changes due to sediment erosion or accretion. This therefore leaves the possibility that data variance is primarily attributable to data ‘noise’ resulting from the inability of the radar and/or the data processing algorithms to capture small waves or waves approaching from certain directions.

To investigate further the effect of wave direction on the quality of the radar data, the spatial distribution of signal return values for waves approaching from northeast and the southeast directions were examined. An animation was created showing time-series of water level and wave height and peak direction concurrently with maps of the signal strength. The analysis of this video indicated that waves approaching from the northeast result in high signal returns in the north sector of the radar images and lower returns in the southern sector (Figure 16A). Similarly, waves approaching from the southeast create high signal returns in the south and lower returns in the north (Figure 16B).

The two examples shown in Figure 16 have (radar-derived) significant wave height > 2 m and correspondingly strong signal return in most of the radar image. In these areas, where signal return is strong, estimates of depth are expected to have reasonable accuracy. However, the accuracy of the depth estimates degrade in areas where signal returns are low, particularly with increasing distance from the radar. Therefore, even when wave conditions are considered ‘good’, the resulting bathymetric maps derived from the data have variable accuracy across the radar field of view.

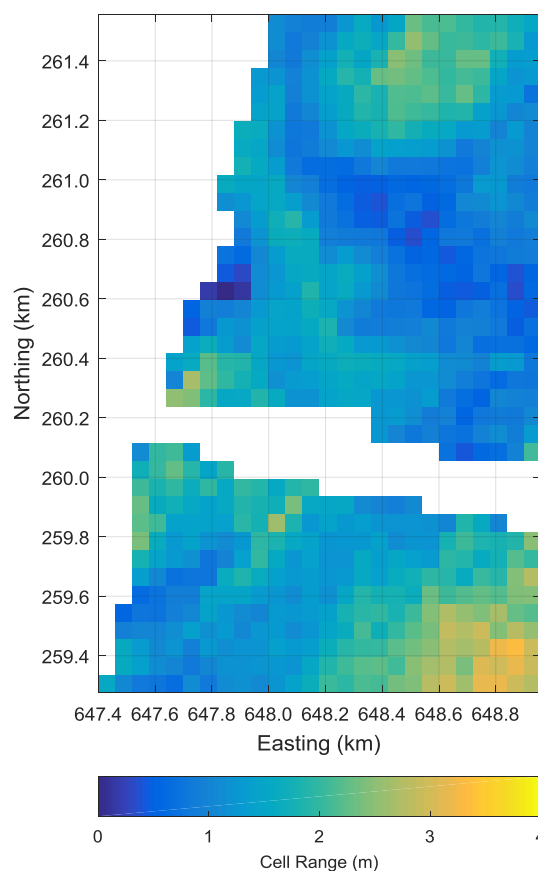


Figure 15. Range of depths derived from radar data captured concomitantly with the multibeam surveys.

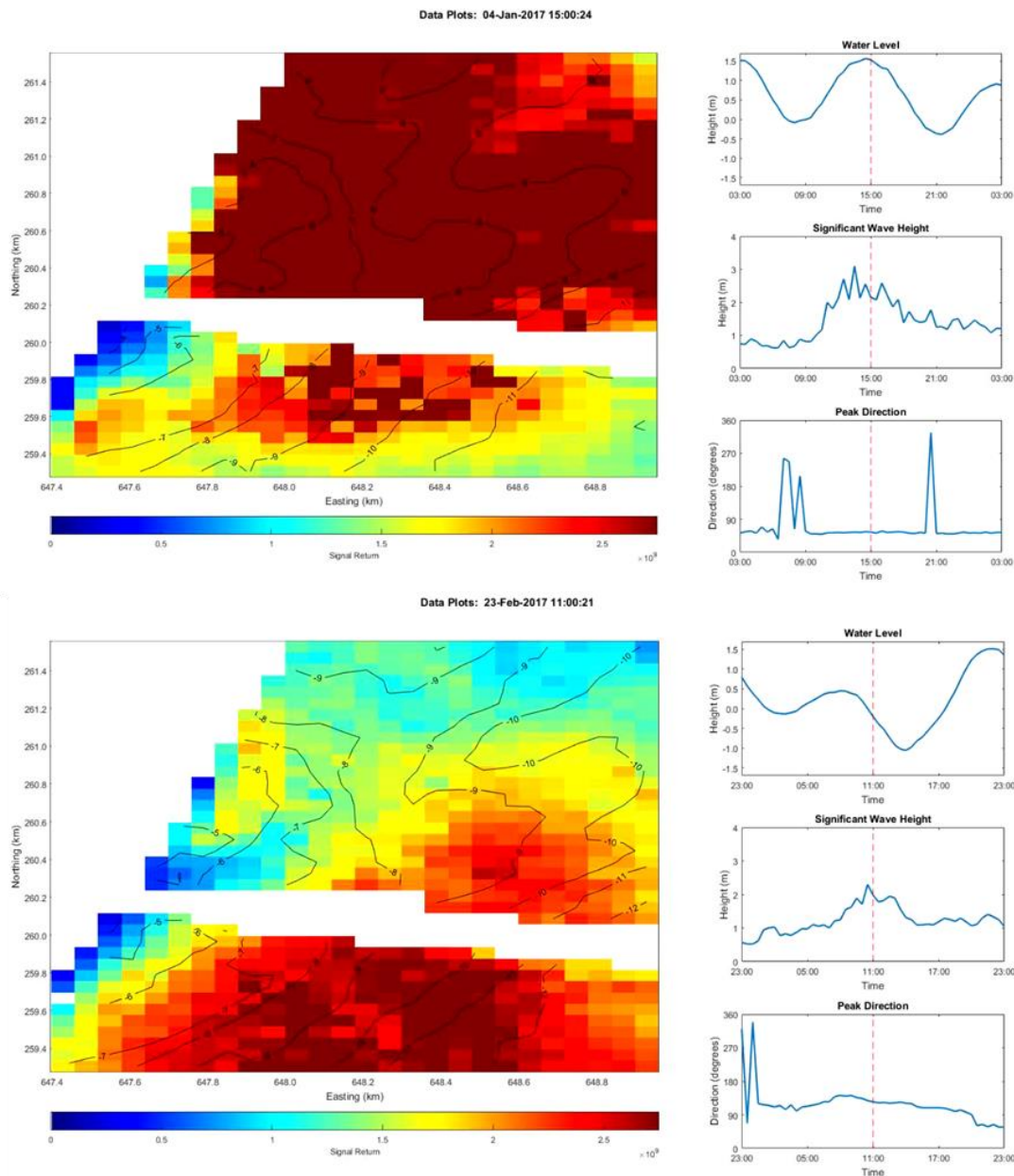


Figure 16. Illustrative examples of the spatial variability in the signal return values of radar data recorded when waves approach from the northeast (A) and the southeast (B). The graphs on the right show radar-derived water levels, significant wave height and peak direction for each example; dashed red lines indicate the conditions at the time corresponding to the images on the left.

This variable wave climate has implications also for the multibeam surveys. Contrary to the radar, the quality of the survey data improves with low wave conditions. Waves can cause excessive pitch and roll and these vessel movements add errors to the data, particularly in surveys undertaken in smaller vessels (commonly used in shallower waters). Unsuitable weather conditions have caused down time of 59.5% and 45.2% for the surveying period of the north and south areas, respectively (Gardline, 2017). Weather conditions are one of the reasons why winter nearshore bathymetry data are rarely available. The radar data in comparison produces higher quality data during wave events. It can then be assumed that the wave conditions in the winter would produce more accurate radar-derived depths than the low wave conditions generally dominant in the summer. However, any resulting changes in bathymetry occurring within the survey period can cause differences between measured and estimated depth and be added as error, even if it reflects a real change.

### APPENDIX 3 – CONSIDERING THE NORTH AND SOUTH SECTORS INDEPENDENTLY

The multibeam surveys in 2017 covered the north and south areas of the radar view at time periods that overlapped but were slightly different (see Appendix 1). Therefore, to identify the best radar record to be used in the linear regression analysis, two options were considered:

1. A composite bathymetry formed by the records showing the highest  $R^2$  value for the south and north sections (13-Jan-17 and 8-Feb-17, respectively) with the LSRL calculated for the composite dataset; and
2. A bathymetry formed by the records showing highest  $R^2$  value when the full radar view is considered (13-Jan-17 02:30).

Figure 17 shows the paired depth values used in the analysis for option 1. For the same measured depth (shown in the horizontal axis), the estimated depth values (shown in the vertical axis) in the north area tend to be higher than the values estimated in the south area. Therefore, the LSRL for the composite dataset (shown in red) would not necessarily be the best fit for any of the two areas, despite a reasonably strong correlation. Option 2 was then considered to reflect the best radar-derived depth values in the period of the multibeam surveys, which were used in the data validation procedure (methods are explained in Section 2.2 and results presented in Section 3.2).

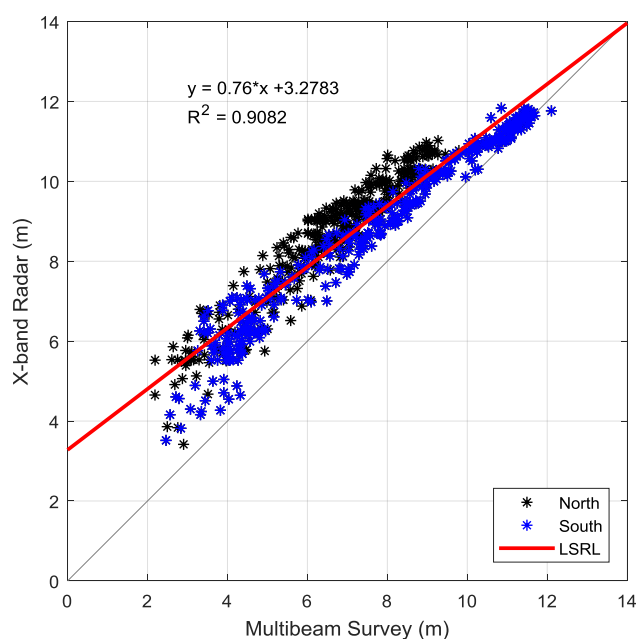


Figure 17. Linear regression analysis of radar-derived depths for a composite dataset represented by the radar record in the south and north sectors showing the best correlation with the maximum depth measurements in the respective grid cell. The LSRL for the composite dataset is shown in red.